Atmospheric Environment 232 (2020) 117485

Contents lists available at ScienceDirect

Atmospheric Environment

journal homepage: http://www.elsevier.com/locate/atmosenv

Influence of zero-burning policy and climate phenomena on ambient $PM_{2.5}$ patterns and PAHs inhalation cancer risk during episodes of smoke haze in Northern Thailand

Nuttipon Yabueng [a], Wan Wiriya [b,c], Somporn Chantara [b,c,*]

[a] PhD Degree Program in Environmental Science, Environmental Science Research Center, Faculty of Science, Chiang Mai University, Chiang Mai, 50200, Thailand
[b] Environmental Science Research Center, Faculty of Science, Chiang Mai University, Chiang Mai, 50200, Thailand
[c] Environmental Chemistry Research Laboratory, Department of Chemistry, Faculty of Science, Chiang Mai University, Chiang Mai, 50200, Thailand

HIGHLIGHTS

- The implementation of the zero-burning policy can reduce open burning activities.
- The policy resulted on $PM_{2.5}$ level reduction but prolonged smoke haze duration.
- ENSO phenomena affects open biomass burning and ambient $PM_{2.5}$ concentrations.
- Diagnostic ratios of some PAHs revealed biomass burning as major source.

GRAPHICAL ABSTRACT

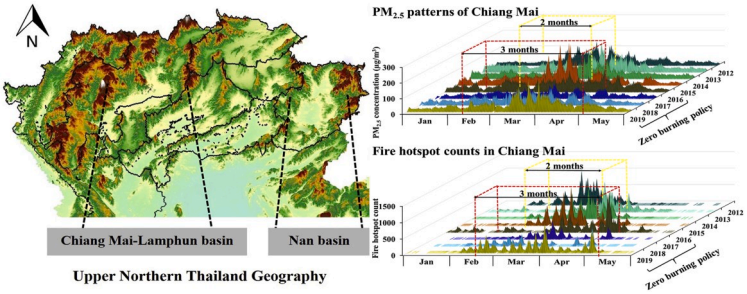

ARTICLE INFO

Keywords:
Air pollution
$PM_{2.5}$
PAHs
Zero-burning policy
Climate impact
Open burning
Carcinogen

ABSTRACT

Air pollution from open burning in the Southeast Asian region has become an important environmental issue in the past decade, mainly due to its impacts on the economy and human health. Daily samples (24-h sampling) of particulate matter having an aerodynamic diameter equal to or less than 2.5 μm ($PM_{2.5}$) were collected during the dry season (March–April) in the years 2017 and 2018 from two sampling sites: one in a suburban area of Chiang Mai Province (CM) that is regularly impacted by forest fires during the dry season, and one near an agricultural residue burning source located in Nan Province (NN). Daily average $PM_{2.5}$ concentrations measured in Chiang Mai from both years (around 38–42 μg/m^3) were about 2 times lower when compared to the same time period prior to the implementation of the zero-burning policy (2012–2015) with an average $PM_{2.5}$ of 67.1 ± 34.1 μg/m^3. Comparisons made during La Niña years (which are usually less affected by open burning), i.e. in 2012 (56 μg/m^3), make it clear that a drop in $PM_{2.5}$ values was influenced by the implementation of the zero-burning policy that was enforced for a period of about 60 days in an attempt to control open burning practices in upper Northern Thailand. Based on the patterns of $PM_{2.5}$ concentrations observed during the dry season, it was determined that the policy could reduce open burning activities during the periods of the policy implementation. However, the zero-burning policy has also contributed to prolonging the smoke haze situation from a 2-month period (mid Feb –mid Apr) to a 3-month-long period (mid Feb–mid May). Moreover, health risks from the inhalation of $PM_{2.5}$ bound PAHs is of great concern. $PM_{2.5}$ concentrations at the two study sites were not significantly different, but average concentrations of 16 PAHs at the NN station for both years (≤ 5 ng/m^3) were

* Corresponding author. Environmental Science Research Center, Faculty of Science, Chiang Mai University, Chiang Mai, 50200, Thailand.
E-mail address: somporn.chantara@cmu.ac.th (S. Chantara).

https://doi.org/10.1016/j.atmosenv.2020.117485
Received 7 December 2019; Received in revised form 3 March 2020; Accepted 6 April 2020
Available online 1 May 2020

higher than those at the CM station (≈ 2 ng/m^3). Therefore, exposure to $PM_{2.5}$ at Nan area was more hazardous than at Chiang Mai. The ratio of some PAHs, i.e. BaA/(BaA + CHR) and IND/(IND + BPER), were used to determine the potential pollutant sources during the dry season, and it was found that $PM_{2.5}$ at both sampling sites probably originated from similar source origins, i.e. wide-spread biomass burning (major source) and traffic emissions (minor source). In addition, not only are fine particulate matters a concern, but their chemical composition, particularly the levels of carcinogenic compounds that are bound to the PMs, are also believed to be a significant cause of these adverse health effects.

1. Introduction

Air pollution has become a serious environmental problem in Southeast Asia (SEA), particularly during the dry season. Open burning involving forest fires and the burning of agricultural residue has been identified as a major source of the worsening air quality in SEA (Chantara et al., 2012). An increase in the amount of air pollutant emissions throughout the entire country has enabled researchers to realize the severity of the adverse health effects associated with air pollution. To be more specific, the upper region of SEA, including Northern Thailand, has experienced a range of severe and worrying impacts that have been associated with the air pollution that results from biomass burning over the past decade. Upper Northern Thailand (UNT) is the area that has been most impacted in Thailand because many of the cities are geographically located within a basin created by the surrounding high mountains. This geographical feature coincides with certain relevant meteorological conditions, including temperature inversion and calming winds that favor the stagnation of air and the accumulation of pollutants. These conditions also limit the dispersion of these pollutants during the dry season (Pani et al., 2018). Apart from that, climate conditions, especially El Niño-Southern Oscillation (ENSO), also contribute to the severity of the air pollution situation in SEA. PM_{10} concentrations and fire hotspot counts reported in Chiang Mai Province during the dry season of 2011 were lower than usual due to the La Niña event (Punsompong and Chantara, 2018; Wiriya et al., 2013). Generally, the effect of La Niña creates conditions that include wetter-than-average rainfall amounts in SEA, while El Niño produces the opposite effect. The government of Thailand has been trying to control the problem by reducing open burning in the affected areas (9 provinces). The "zero-burning" plan was therefore implemented as a strategic initiative in 2013 and introduced to the entire area of UNT during the dry season (February to April). However, strict implementation and legal enforcement of the policy has only occurred since 2016. This policy was announced by the acting governor to control open burning in UNT (9 provinces) for a period of about 60 days from February to April each year. Fire hotspot counts in the dry season of 2017 and 2018 that were detected by satellite remote sensing imagery provided by the Visible Infrared Imaging Radiometer Suite (VIIRS) decreased by 50–80% from the past 10-year average values. This outcome likely would have occurred as a result of the zero-burning policy and/or certain other factors such as the relevant metrological conditions (i.e. precipitation, relative humidity and wind speed). Air pollution is recognized as a transboundary form of pollution; therefore, policies intended to control burning in specific regions might not be effective in terms of the prevention of air pollution throughout the greater region. Fine inhalable particles with a diameter that is equal to or less than 2.5 μm ($PM_{2.5}$) meet the criteria for pollutants that are most hazardous. This particulate matter is currently among the most widespread health threats because these particles can penetrate more deeply into the human respiratory tract than coarser particles (Liu et al., 2017). Additionally, these particles can adsorb various other toxic organic compounds, especially polycyclic aromatic hydrocarbons (PAHs), that can induce free-radical species production which may contribute to the formation of oxidative DNA lesions and ultimately lead to the formation of mutagenic DNA adducts (Castellano et al., 2003; Danielsen et al., 2009; Feilberg et al., 2001; Schnelle-Kreis et al., 2001).

PAHs are mainly generated from incomplete combustion processes associated with a number of humans activities, such as fossil fuel combustion, coal and coke combustion, biomass burning, traffic emissions and oil spills (Zhang and Tao, 2009). About 80% of particle-bound PAHs are attributed to $PM_{2.5}$, while PAH concentrations are highly dependent upon these fine particles (Duan et al., 2007; Hassanvand et al., 2015). Generally, low molecular weight or 2–3-ring PAHs are particularly dominant in the gas phase, while those with 4 or more rings are generally more dominant in the particulate phase (Hanedar et al., 2011; Ravindra et al., 2008). The PAHs that are recognized as carcinogenic are mostly associated with particulate matter (Bi et al., 2003; Ravindra et al., 2008; Wiriya et al., 2013). It has been reported that 80% of PAHs disrupt the alveoli and 20% impact upon the tracheobronchial region of the respiratory tract (Sarigiannis et al., 2015). However, deeper regions of the respiratory system tend to be more affected by the ultimate doses of more toxic substances and their carcinogenic metabolites. This is because of the lower rates of diffusion that occur through the bronchial epithelium. PAH metabolites may later alter the replication and transcription mechanisms of DNA and induce tumors (Armstrong et al., 1994; Boström et al., 2002). Health risk assessments can be calculated from the toxicity equivalent concentration (TEQ) based on PAHs concentrations and toxic equivalent factors (TEFs) (TEF of benzo[a]pyrene is equal to 1) (Nisbet and Lagoy, 1992). In addition, the PAHs emission profile of each process can help to identify the origin of the contamination (Manoli et al., 2004). Diagnostic ratios are a tool that can be used to classify the qualitatively distinguishing petrogenic and pyrolytic sources by comparing the ratio of individual PAHs concentrations with other relevant well-known references (i.e. fluoranthene (FLA), pyrene (PYR), benzo[a]anthracene (BaA), Chrysene (CHR), indeno [1,2,3-cd] pyrene (IND), benzo[g,h,i]perylene (BPER), anthracence (ANT), phenanthrene (PHE), benzo[a]pyrene (BaP), etc.) (Wang et al., 2017). Thus, the study of PAHs in $PM_{2.5}$ can lead to the provision of useful tools for environmental monitoring, source identification and health risk assessments.

This study aims to (i) evaluate the impacts of the zero-burning policy as well as the climate conditions associated with the patterns of $PM_{2.5}$ concentrations, (ii) compare and identify possible sources of $PM_{2.5}$-bound PAHs occurring from different land-use areas (suburban areas and areas near biomass burning sources), and (iii) evaluate human health risks from PAHs based on toxicity equivalent concentrations (TEQs) and assess the inhalation cancer risk (ICR).

2. Methodology

2.1. Characteristics of study sites

Northern Thailand consists of 17 provinces covering 169,600 km^2 (≈ 33% of Thailand). The upper part of the area (≈ 100,000 km^2) is our target study area because of its specific geographic conditions, i.e. basins surrounded by mountain ranges as well as a variety of land use patterns. The greater area is comprised of ~ 65% forest land and ~ 30% agricultural areas. Two sampling sites were selected; one in the sub-urban area of Chiang Mai (CM) Province (the western part of UNT), and one in the rural area of Nan (NN) Province (the eastern part of UNT) (Fig. 1).

The city of Chiang Mai is the largest urban area in northern Thailand and is also one of the most popular tourist cities in Thailand with a

population of 1.7 million contained within a total area of 22,000 km^2. The geography of Chiang Mai consists of mountains positioned in a north-south direction that are covered with deciduous forests. CM station therefore was selected because it is situated close to forest burning sources. The sampling site was located in a suburban area at the meteorological station in the area of Mea Hia Research Center, Chiang Mai University, Muang District, Chiang Mai Province, Thailand. Compared with the CM site, the NN site was selected for its proximity to sources of agricultural residue burning. In terms of agriculture, crop raising areas in UNT are now particularly dedicated to the maize crop, while Nan Province has the largest area of maize plantation (17% of total area of UNT). In addition, most of the active fires have been detected during the dry season in Nan Province over the last 10 years. The NN site is located in a rural area at Ban Nong Ha Primary School, Na Noi District, Nan Province.

2.2. $PM_{2.5}$ sample collection

Ambient $PM_{2.5}$ samples were collected every day for 24 h on a 47 mm quartz-fiber filter (QM/A, Whatman Inc., UK) using a low volume air sampler (PQ200) with a flow rate of 16.7 L/min during the dry seasons (March–April) of 2017 and 2018. Before sampling, the filters were stored in a desiccator for 24 h to remove any moisture and were then pre-weighed three times on an MX-5 microbalance (Mettler Toledo, Switzerland) under conditions of controlled temperature (24.5 ± 0.7 °C) and relative humidity (31 ± 2%). After sample collection, the filters were kept on an aluminum foil plate and then transferred into a desiccator for 24 h before being re-weighed and stored at −20 °C until analysis. The numbers of samples collected were 114 and 69 for the years 2017 and 2018, respectively.

2.3. $PM_{2.5}$-bound PAHs analysis

$PM_{2.5}$-bound PAHs were extracted and analyzed for their potential health risk. Sixteen-EPA PAHs were the main focus of this study according to their carcinogenic potential. The $PM_{2.5}$ samples were extracted in 25 mL of mixture solvent (dichloromethane: hexane (1:1, v/v)) using an ultrasonicator for 45 min at a controlled temperature (below 10 °C). The extraction solutions were then filtered through a 0.45 μm nylon filter (Agela Technologies, USA) prior to being

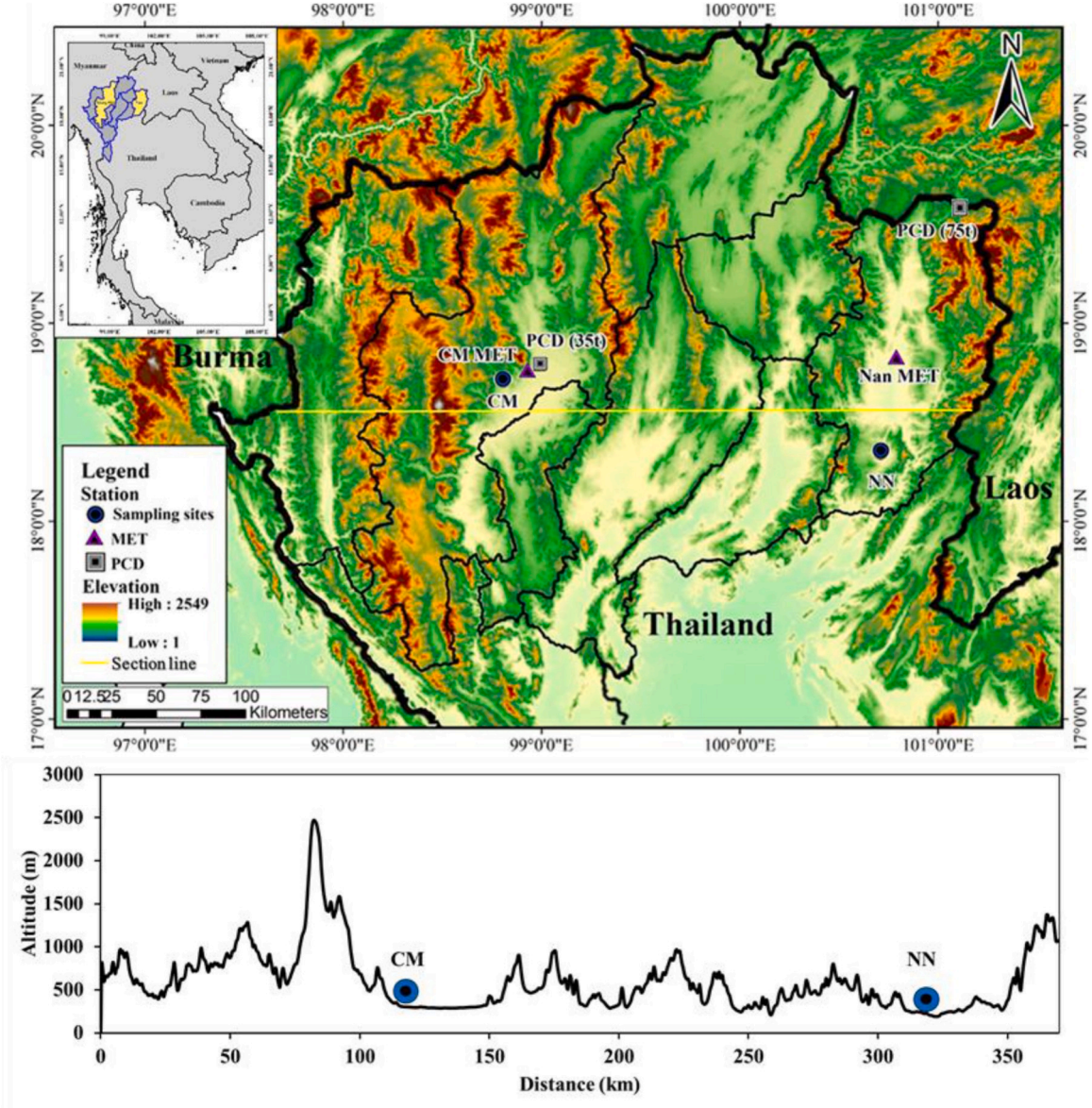

Fig. 1. Geographical domain of UNT and location of CM and NN stations.

evaporated by vacuum rotary (vacuum pressure 300–80 mbar at a speed of 85 rpm) until they were nearly dried. A mixture of internal standards (acenaphthene-d10 and perylene-d12) was spiked into the extracted solution and it was adjusted to 2 mL by adding the aforementioned mixture solvent (Bootdee et al., 2016). PAHs were then analyzed by gas chromatography–mass spectrometry (GC-MS) using an Agilent 7820A gas chromatograph coupled to an Agilent 5977E. The instrument was equipped with a HP-5MS UI capillary column (30 m × 0.25 mm × 0.25 μm). The oven temperature program for the analysis of PAHs was as follows: 70 °C for 2 min, increased to 200 °C at a rate of 8 °C/min and held for 2 min, to 260 °C at 10 °C/min for 8 min and increased to 290 °C at 15 °C/min and held for 7 min. The carrier gas was high-purity helium. The detection mode was operated in the selective ion monitoring (SIM) mode. Target PAHs, including naphthalene, acenaphthylene, acenaphthene, fluorene, phenanthrene, anthracene, fluoranthene, pyrene, benz[a]anthracene, chrysene, benzo[b]fluoranthene, benzo[k]fluoranthene, benzo[a]pyrene, indeno[1,2,3-cd]pyrene, dibenz[a,h]anthracene, and benzo[g,h,i]perylene, were identified.

2.4. Quality assurance and quality control for GC-MS analysis

The limit of detection (LOD) values of GC-MS were identified with seven injections of the lowest concentration (1 ng/mL) of 16 PAHs mixed standard used for construction of the corresponding calibration curves. LOD values were calculated from three multiplications of the standard deviation (SD) of the seven injections of each PAH. The LOD values for the individual PAHs compounds ranged from 0.062 to 0.461 ng/mL. The accuracy of the PAHs analysis was determined by Standard Reference Material (RSM) urban dust 1649b (National Institute of Standard & Technology; NIST) and by the spiking of the mixed standard (2 ng/mL of final concentration) on a quartz filter prior to extraction. Three sets of about 50 mg SRM and the spiked filter were extracted using the same method as the samples. Percentage recoveries of 14-PAHs (91–188%) were obtained from SRM and the percentage recoveries of all species (78–94%) were obtained from the spike method (Table 1). Moreover, low percentage relative standard deviation (RSD) was obtained between 2 and 14%, which confirmed the relatively high degree of accuracy and reproducibility of the analysis.

2.5. PAHs source identification using diagnostic ratio

Diagnostic ratio is a tool for identification possible sources of PAHs using the isomeric ratios. The isomeric ratios are concentration ratios of some individual PAHs considering as fingerprint of an emission source (Khalili et al., 1995). The ratios of PAHs isomer have been widely used to identify particular source of $PM_{2.5}$-bound PAHs.

2.6. Analysis of fire hotspots and air mass movement

2.6.1. Fire hotspots

Fire hotspots provided by the Fire Information for Resource Management System (FIRM) were investigated in high-resolution satellite images from the Visible Infrared Imaging Radiometer Suite (VIIRS).

2.6.2. Analysis of air mass movement using backward trajectory

Two-day backward trajectories (BWTs) arriving at the receptors (CM and NN stations) were computed using Hybrid Single-Particle Lagrangian Integrated Trajectory (HYSPLIT) model. Global Data Analysis System (GDAS) meteorological data (1.0° × 1.0°) were used for calculations of daily trajectories for 2 months (March–April) of the years 2017 and 2018, stating at 00, 06, 12 and 18 UTC (07.00, 13.00, 19.00 and 01.00 local time) from altitudes of 10 m above ground level (AGL).

2.7. Health risk assessment in relation to PAHs

2.7.1. Toxicity equivalent concentration (TEQ)

The toxicity equivalent concentration (TEQ) equation was improved by US EPA and widely used to estimate risk of PAHs inhalation. It can be calculated as Eq. (1)

$$TEQ = \sum [PAH_i \times TEF_i] \quad (1)$$

Here, PAH_i is representative of an individual PAHs concentration and TEF_i is representative of the toxic equivalent factors. TEF therefore is an

Table 1
Characteristics of 16 PAHs, method detection limits (MDLs) and percentage extraction recovery of 16 PAHs from spike method.

PAHs	Abbreviation	Ring number	Carcinogenic group[a]	Quantification ion (m/z)	LOD (ng/mL) (n = 7)	MDLs (ng/m^3) (n = 7)	Recovery (%) (n = 3)		RSD (%) (n = 3)
							SRM	Spiked	
Low molecular weight									
Naphthalene	NAP	2		128	0.241	0.020	–	89	12
Acenaphthylene	ACY	3		152	0.110	0.009	–	86	5
Acenaphthene	ACE	3		154	0.110	0.009	–	90	4
Fluorene	FLU	3		166	0.062	0.005	–	84	3
Phenanthrene	PHE	3		178	0.084	0.007	91	78	10
Anthracene	ANT	3		178	0.184	0.016	135	85	12
High molecular weight									
Fluoranthene	FLA	4		202	0.159	0.013	111	85	9
Pyrene	PYR	4		202	0.207	0.018	121	81	10
Benz[a]anthracene	BaA	4	2B	228	0.116	0.010	101	78	12
Chrysene	CHR	4	2B	228	0.166	0.014	99	82	14
Benzo[b]fluoranthene	BbF	5	2B	252	0.217	0.018	100	87	5
Benzo[k]fluoranthene	BkF	5	2B	252	0.151	0.013	126	93	6
Benzo[a]pyrene	BaP	5	1	252	0.461	0.039	94	93	6
Indeno[1,2,3-cd] pyrene	IND	6	2B	276	0.414	0.035	152	93	11
Dibenz[a,h] anthracene	DbA	5	2A	278	0.459	0.039	188	94	10
Benzo[g,h,i]perylene	BPER	6		276	0.300	0.025	112	88	2

[a] International Agency for Research on Cancer: carcinogenic to humans (Group 1), probably carcinogenic to humans (Group 2A) and possibly carcinogenic to humans (Group 2B)*Italic* is Carcinogenic PAHs (cPAHs).

estimate of the associated toxicity of chemicals in comparison to the BaP, which is a reference compound (Nisbet and Lagoy, 1992). The other PAHs, which had lower potency levels than BaP, were assigned to different TEF values. Three equations of TEQ based on previously established experiments (Nisbet and Lagoy, 1992) (Eq. (1.1)), (U.S.EPA, 1993) (Eq. (12)), and (Cecinato, 1997) (Eq. (1.3)) were used in this study.

$$\text{TEQ} = 0.001(\text{NAP} + \text{ACY} + \text{ACE} + \text{FLU} + \text{PHE} + \text{FLA} + \text{PYR}) + 0.01(\text{ANT} + \text{BPER} + \text{CHR}) + 0.1(\text{BaA} + \text{BbF} + \text{BkF} + \text{IND}) + \text{BaP} + \text{DBA} \quad (1.1)$$

$$\text{TEQ} = 0.06(\text{BaA}) + 0.07(\text{BbF} + \text{BkF}) + \text{BaP} + 0.08\ (\text{IND}) + 0.6\ (\text{DBA}) \quad (1.2)$$

$$\text{TEQ} = 0.01(\text{CHR}) + 0.1(\text{BaA} + \text{BbF} + \text{BkF} + \text{IND}) + \text{BaP} + \text{DBA} \quad (1.3)$$

2.7.2. Inhalation cancer risk (ICR)

The inhalation cancer risk (ICR) was used to estimate the genotoxic effects from PAHs exposure. The proposed equation (U.S.EPA, 2005) is presented in Eq. (2).

$$ICR = TEQ \times IUR_{BaP} \quad (2)$$

Here, IUR_{BaP} is the inhalation unit of risk defined as the risk of cancer from a lifetime (70 years) of halation of the unit mass of BaP, which is recommended as 8.7×10^{-2} $m^3/\mu g$ by the World Health Organization (WHO, 2000) and 1.1×10^{-3} $m^3/\mu g$ by the Office of Environmental Health Hazard Assessment (OEHHA) of California Environmental Protection Agency (CalEPA) (OEHHA, 2003), respectively.

3. Results and discussion

3.1. Patterns of ambient $PM_{2.5}$ concentrations in UNT and impact of zero-burning policy

3.1.1. Patterns of $PM_{2.5}$ concentrations during smoke haze season

Smoke haze episodes usually occur in the dry season (February–April) over the upper region of Southeast Asia. In this study, daily $PM_{2.5}$ samples were collected from two sampling sites located in UNT during the dry seasons of the years 2017 and 2018 for further chemical composition analysis. In order to test the data quality of the sampling results, $PM_{2.5}$ concentrations were plotted with data obtained from Beta Ray Attenuation measurements conducted at Air Quality Monitoring (AQM) stations belonging to the Pollution Control Department (PCD) of Thailand. These stations were situated in the city of Chiang Mai (35t) and Chaloemprakiat District, Nan Province (75t). Strong correlations ($r > 0.90$) between $PM_{2.5}$ concentrations at the CM station and PCD (35t) were observed in both years confirming a degree of data similarity between the two locations (≈ 9 km distance) and the two measuring techniques that were employed. Meanwhile, in Nan Province, the correlation was found to be moderate ($r = 0.6$–0.8). The main reason for this was probably due to the substantial distance (≈ 141 km) between the two locations (sampling site in Na Noi District and PCD station (75t) in Chaloemprakiat District). Due to the limitation associated with the eastern area, $PM_{2.5}$ data were only available from this station. During the open burning season, or the so-called "smoke haze" season, the patterns of PM concentrations of all stations in UNT were similar. However, the concentration levels may have varied due to micro-environmental factors, i.e. local activities and local weather conditions.

Plots of distribution of daily average $PM_{2.5}$ data obtained from the CM-AQM station (PCD_36t) during the period from 2012 to 2015 are shown in Fig. 2. The patterns of PM concentrations that were monitored

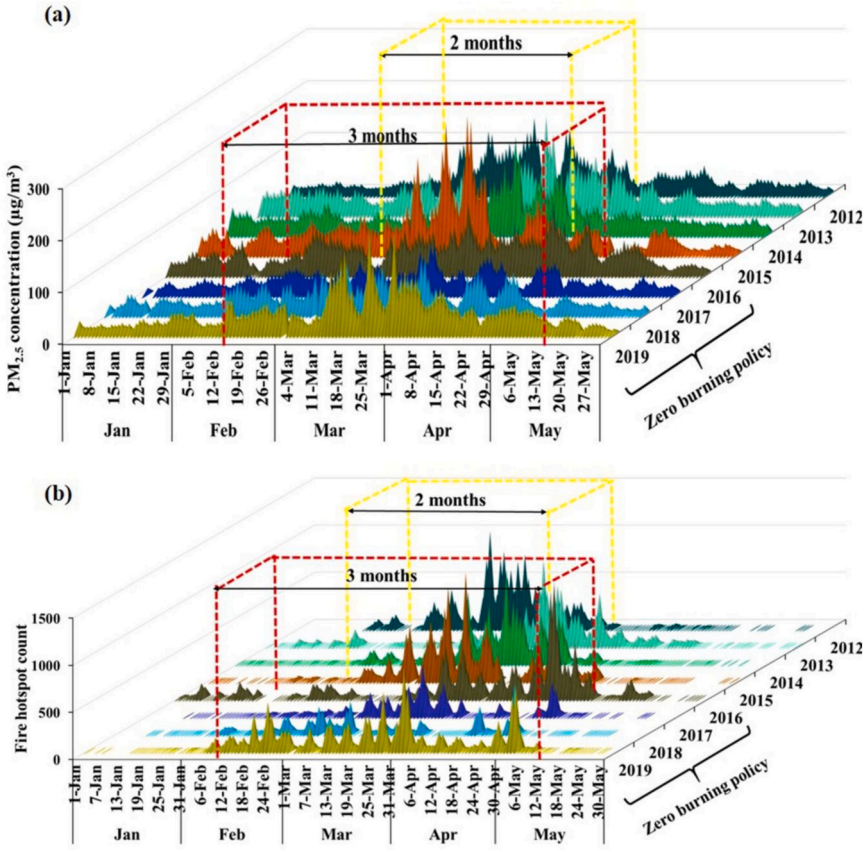

Fig. 2. Patterns of daily $PM_{2.5}$ concentrations in the city of Chiang Mai (a) and fire hotspot counts in Chiang Mai Province (VIIRS) (b) from 2012 to 2019.

in the city of CM for the 4-year period of data collection revealed similar patterns (Fig. 2a). $PM_{2.5}$ concentrations began to increase at around the middle of February and reached its peak in March before decreasing by the middle of April. Interestingly, it was found that the pattern of $PM_{2.5}$ concentrations during the dry season from 2016 to 2018 changed when compared to the previous annual pattern. No sharp peak was found in March as usual, but the PM levels fluctuated and presented as a flat curve during the period from February to May. The PM patterns in 2017 and 2018 in CM were similar to the pattern observed in 2016 (the first year of the implementation of the zero-burning policy) (Fig. 2a). This policy has been conscientiously implemented since 2016 by the Thai government in order to control open burning practices (i.e. forest fires, agricultural burning and garbage burning) in 9 provinces of UNT in the dry season (from mid-February to April). The duration of this policy is about 60 days, but the beginning and the end can vary from one province to another depending on land use, micro-climate conditions and fire hotspot data collected from previous years. The $PM_{2.5}$ pattern in 2019 was different from that of the years from 2016 to 2018, but was similar to that of the years from 2012 to 2015. The peak was observed during the middle of March to April in 2019. When comparing the $PM_{2.5}$ patterns of the years with similar climate conditions (2016 and 2019, which were the El Niño years), it was found that the patterns were totally different (Fig. 2a). This outcome may have resulted from the transboundary haze pollution originating from a south west direction (Mea Hong Son Province and Myanmar). Fig. 2b shows the distribution of fire hotspots during the years of January to May in the years from 2012 to 2019. The data can be divided into two groups; (i) years before implementation of the zero-burning policy (2012–2015) and (ii) years of the implementation of the zero-burning policy (2016–2019). During the years of 2012–2015, the distribution of the number of open burning (fire hotspot count) was related to the $PM_{2.5}$ concentration pattern (peak recorded in March). During the years of implementation of the policy (2016–2019), the fire hotspot count in March was lower than the previous years and the peak (highest number of hotspots) was delayed by about 1 month when compared with the pattern recorded during the years from 2012 to 2015. Moreover, $PM_{2.5}$ concentrations and the fire hotspot count during the years from 2016 to 2019 were relatively weakly correlated. In order to assess the effectiveness of policy implementation on $PM_{2.5}$ concentrations, the years with similar climate conditions (i.e. La Niña years including 2012, 2017 and 2018) were selected. It was found that the average $PM_{2.5}$ concentrations during the years from 2017 to 2018 (weak La Niña years) were about 10% lower than of 2012 (moderate La Niña year). Moreover, the average $PM_{2.5}$ concentrations decreased by about 20% and 36% in the years from 2013 to 2014 (neutral year) and 2015 (weak El Niño year), respectively. Apart from the policy implementation, global climate phenomena (El Niño and La Niña) are a crucial factor that affects the air pollution situation in this area. Although a zero-burning policy was implemented in the years 2016 and 2019 (El Niño years), the average $PM_{2.5}$ concentrations were still higher than in 2017 and 2018. According to the aforementioned patterns and concentration levels, it can be concluded that the zero-burning policy in UNT was indeed effective in some years and could influence patterns of $PM_{2.5}$ concentrations. Apart from the zero-burning policy, climate patterns can also play an important role in incidences of open burning. Table 2 shows the relevant climate conditions including the El Niño–Southern Oscillation (ENSO) cycle and the total amount of rainfall. The ENSO cycle, which can present fluctuations in temperature between the ocean and the atmosphere in the east-central Equatorial Pacific region, is a major meteorological condition with an effect on the loading of biomass burning (Hamburger et al., 2013; Punsompong and Chantara, 2018). Generally, ENSO episodes vary between dry episodes (El Niño) and wet episodes (La Niña) over SEA. During the years from 2017 to 2018, the climate conditions were classified as a weak La Niña occurrence. This involved a high amount of precipitation combined with high humidity levels (https://www.ggweather.com/enso/oni.htm). These conditions were considered unfavorable for biomass burning. Therefore, fire hotspot counts (VIIRS) in the UNT area during the period of February–April of 2017 (47,358) and in the year 2018 (37,562) were significantly lower than in the El Niño years, i.e. 2015 (70,351), 2016 (78,979) and 2019 (79,766) (Fig. 5a and b).

3.1.2. *Pattern of $PM_{2.5}$ concentrations, fire hotspot count and meteorological conditions during 2017–2018 at two study sites*

Daily average concentrations of $PM_{2.5}$, rain amounts and fire hotspot counts recorded during the open burning season (March to April) of the years 2017 and 2018 were plotted and are shown in Fig. 3. During a three month period, data collection periods can be divided into two subperiods (I: during the preventive action of open burning and II: after the preventive action). During the sub-period I of year 2017, three peaks of $PM_{2.5}$ were found within a similar timeframe at both locations (Fig. 3a and b). In 2018, the fire hotspot counts in the greater UNT area sharply increased on 12 April (2,476). About 70% of the total hotspots were detected in Tak Province (64%) (south and southwest of CM and NN stations, respectively) and Lampang Province (9%) (southeast and south of CM and NN stations, respectively). In fact, the implementation of the zero-burning policy in these two provinces ended earlier (April 10, 2018) than in other provinces. It can be clearly seen that the policy implementation was effective within these years. Afterwards, burning activities began again and $PM_{2.5}$ concentrations increased in the subperiod I of both study locations. Moreover, the pattern of $PM_{2.5}$

Table 2
Association of global climate, zero-burning period, fire hotspot counts and micro-environment condition (amount of rain) in Northern Thailand in dry season of year 2012–2019.

[a]ENSO type	Year	Zero-burning period		[b]$PM_{2.5}$ concentration (μg/m^3) in CM (Feb–Apr)	[c]Fire hotspot count (Feb–Apr)			[d]Total rain (No. of rainy days) (mm)			
		CM	NN		CM	NN	UNT	CM		NN	
Moderate La Niña	2012	–	–	56.08 ± 30.76	14,614	11,300	77,417	84.2	(11)	357.8	(14)
Neutral	2013	–	–	64.39 ± 32.55	12,593	9283	67,995	49.9	(12)	32.1	(10)
Neutral	2014	–	–	60.28 ± 33.76	16,148	8724	78,534	40.8	(7)	98.2	(18)
Weak El Niño	2015[e]	15 Feb - 15 Apr	1 Feb - 1 Apr	78.91 ± 53.31	16,025	7507	70,351	81.3	(12)	208.5	(16)
Very strong El Niño	2016	16 Feb - 15 Apr	1 Feb - 31 Mar	70.04 ± 23.99	16,427	7803	78,979	63.0	(5)	76.3	(6)
Weak La Niña	2017	20 Feb - 20 Apr	15 Feb - 15 Apr	44.23 ± 17.10	7823	3507	47,358	53.1	(10)	120.5	(11)
Weak La Niña	2018	1 Mar - 20 Apr	15 Feb - 15 Apr	56.88 ± 20.62	6214	2649	37,562	46.9	(18)	177.6	(20)
Weak El Niño	2019	1 Mar - 30 Apr	15 Feb - 15 Apr	65.89 ± 38.44	14,736	7954	79,766	22.3	(4)	81.3	(11)

[a] ENSO types based on the Oceanic Niño Index (ONI) which NOAA uses for identifying El Niño (warm) and La Niña (cool) events in the tropical Pacific (February–April).
[b] Average daily $PM_{2.5}$ concentrations from PCD AQM station (36t) in the city of Chiang Mai.
[c] Fire hotspot counts detected by VIIRS.
[d] Rain data collected during February–April each year obtained from Chiang Mai and Nan Meteorological stations.
[e] In 2015, zero-burning concept is only a strategy plan which is not strict as other years.

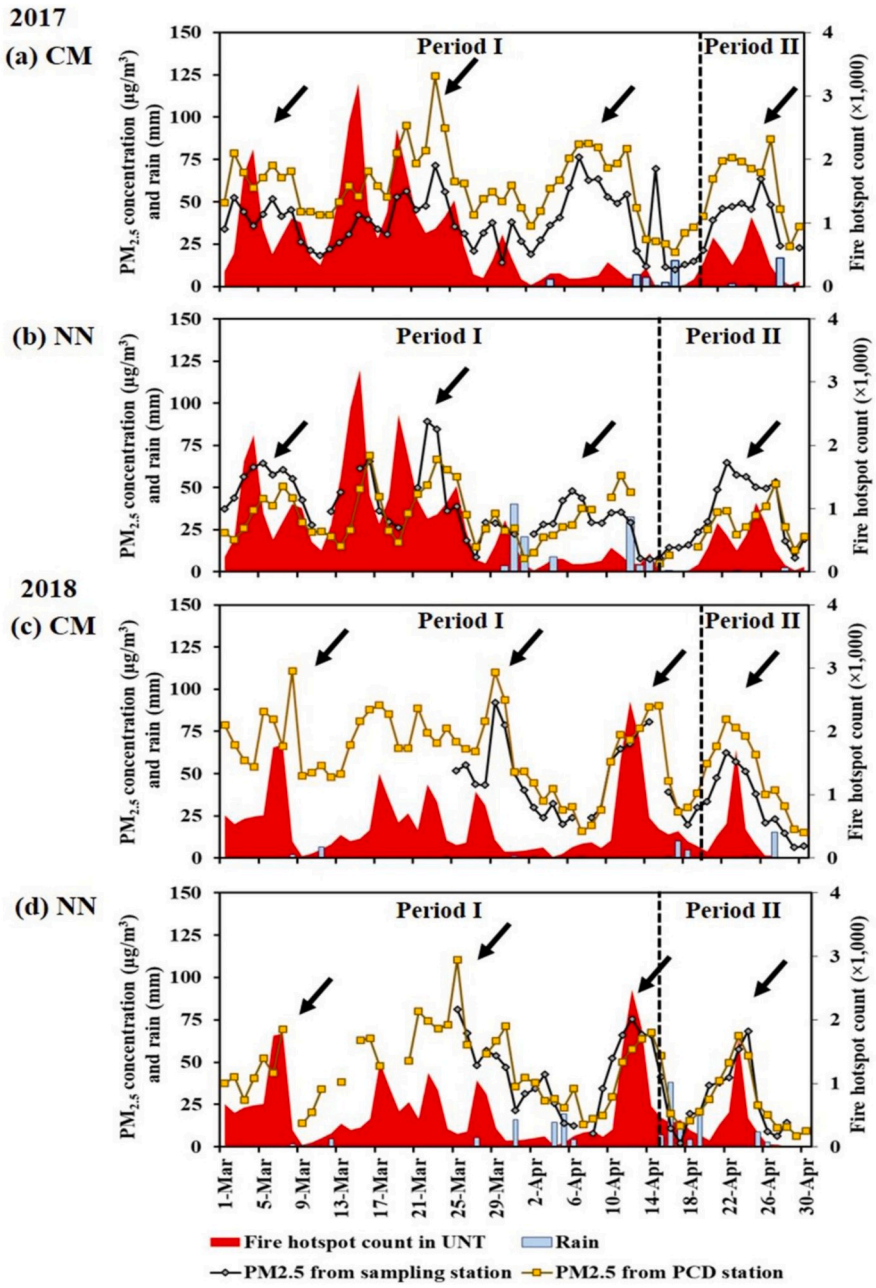

Fig. 3. Daily $PM_{2.5}$ concentrations (μg/m^3) obtained from sampling and PCD stations, fire hotspot counts in UNT (detected by VIIRS) and rainfall of each station in two year period (a) CM station, 2017, (b) NN station, 2017, (c) CM station, 2018 and (d) and NN station, 2018. Arrows show peaks of $PM_{2.5}$ found during sampling periods.

concentrations recorded in 2018 was similar to that of 2017, but the peaks were slightly delayed when compared to previous years (Fig. 3c and d). An association between $PM_{2.5}$ values and the count of fire hotspots was obviously seen in sub-period II (after the end of the preventive action). A peak in $PM_{2.5}$ concentrations was found again on 25 April and the level then decreased during the rainy season (May–October). The average $PM_{2.5}$ mass concentrations measured at the CM station (38.25 ± 16.05 μg/m^3 (2017) and 41.86 ± 21.64 μg/m^3 (2018) were slightly higher than those measured at the NN station (37.93 ± 19.11 μg/m^3 (2017) and 38.11 ± 22.49 μg/m^3 (2018)). However, they were not significantly different in terms of the locations and the years of measurement for the study period. Noticeably, around 20–40% of the daily average $PM_{2.5}$ concentrations from both sampling sites for these two years exceeded the Thailand National Ambient Air Quality Standard (NAAQS = 50 μg/m^3), while more than 65% exceeded the guidelines set by the WHO (25 μg/m^3).

Fig. 4 shows the meteorological parameters, i.e. relative humidity, amount of rain and wind speed, obtained from meteorological stations located near the sampling sites. $PM_{2.5}$ concentrations and fire hotspot counts were also plotted for comparison with changing meteorological data. Wind speed and relative humidity are relevant parameters that were obviously different between these two locations. Wind speed at the CM station (22.8 ± 7.2 km/h) was about 2 times stronger than at the NN station (9.2 ± 3.3 km/h). Kim et al. (2015) reported that PAHs concentrations recorded in the roadway environment decreased in association with conditions of high wind speed (>7.2 km/h). Moreover, Wang et al. (2016) found that the contributions of local activities, such as increased traffic volume, were found to increase concentration values by approximately 2 times when wind speed changed from high (>7.2 km/h) to low (<7.2 km/h) along with the $PM_{2.5}$-bound PAHs

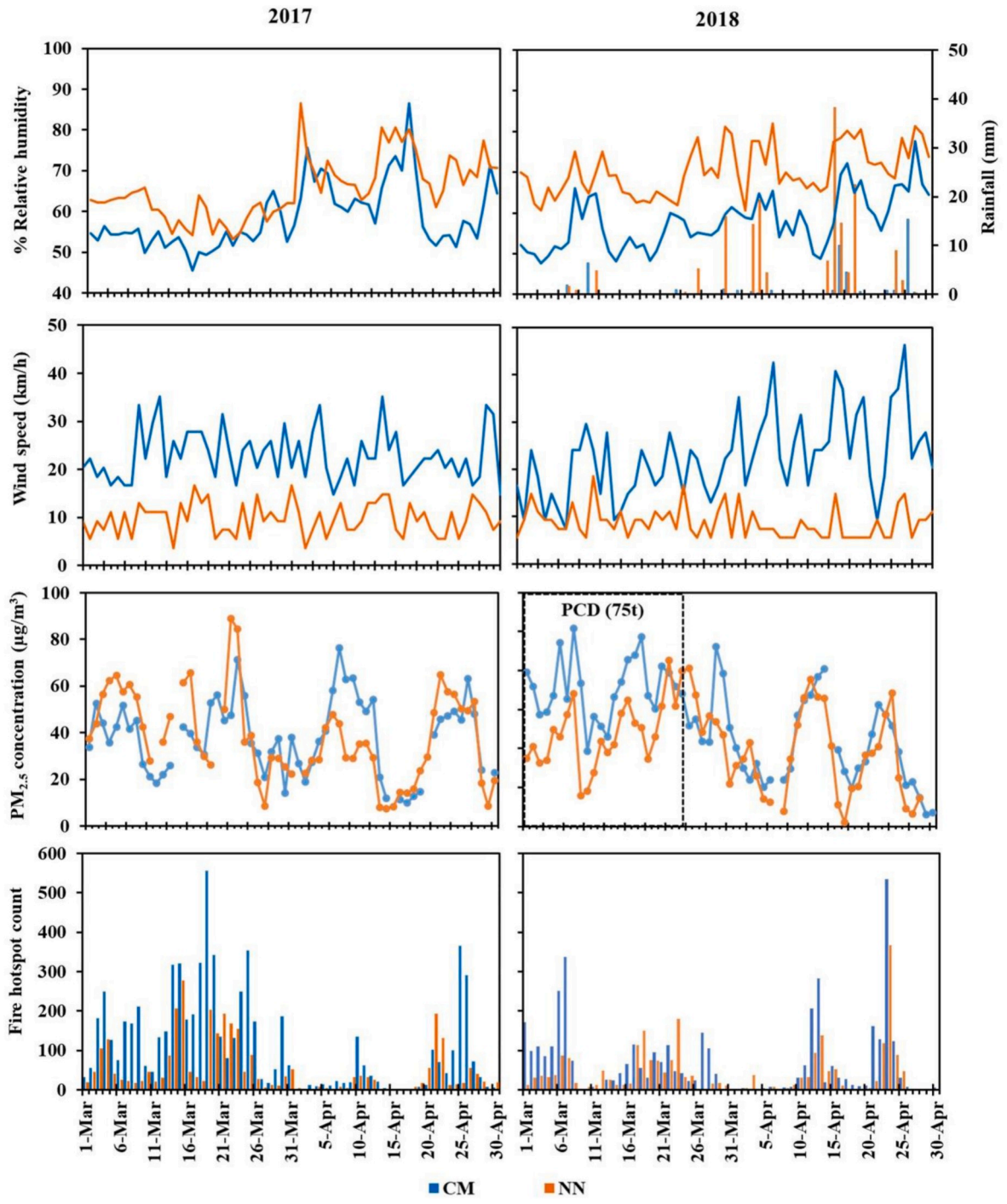

Fig. 4. Variation of meteorological parameters, $PM_{2.5}$ concentration and fire hotspot count (detected by VIIRS) during dry season (March–April) of 2017 and 2018 over Chiang Mai and Nan Province.

concentration values. Chantara et al. (2019) revealed that no significant differences were observed in terms of the emission factors of $PM_{2.5}$ occurring from biomass burning in Northern Thailand, except for the high emission factors associated with some of the water soluble ions (K^+ and Cl^-) present in the agricultural biomass. Hence, meteorological conditions, particularly wind speed and different kinds of biomass burning, might have an influence on PAHs levels.

In terms of topography, both locations were similar. However, the Chiang Mai-Lamphun basin, where the CM station is located, is obviously larger and deeper when compared to the Nan basin (Fig. 1). During high pressure conditions, air pollutants are accumulated and trapped in the basin. Ground wind speed is an important factor in dispersing pollutants out of a basin area. According to the wind speed recorded during the haze season, air pollutants in the Chiang Mai-Lamphun basin can be dispersed more effectively than those in the Nan basin, although the former was still surrounded by high mountains. In addition, the relationship between land use activities (supplement), burned areas and air mass trajectory values (Fig. 5) were considered critical in providing more in-depth information on pollutant sources. During the dry season, a high density of fire hotspots could be detected over SEA. This shows that open burning occurs all across this region. In Thailand, the majority of the burning occurred in forest and agricultural areas. In this study, 2-

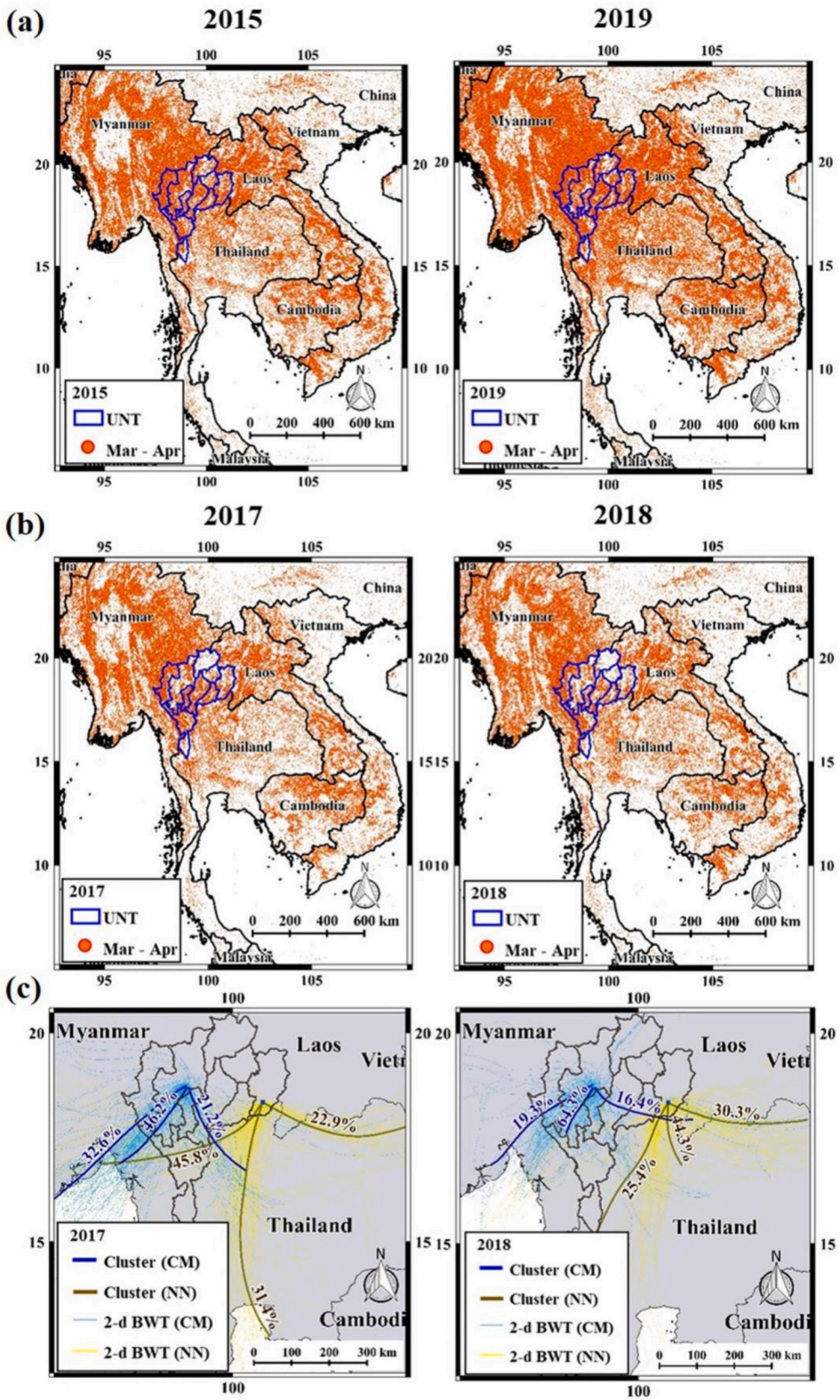

Fig. 5. Comparison of active fire hotspots (detected by VIIRS) in SEA during dry season (March–April) between (a) El Niño year (2015 and 2019) and (b) La Niña year (2017 and 2018) and (c) 2-day backward trajectories (air mass movement) arriving at CM and NN stations at 10 mAGL (average between 7AM, 1PM, 7PM and 1AM local time).

day backward trajectories of the arrival of air mass movements at the sampling stations during the dry season (March–April 2017 and 2018) were analyzed. The direction of the air mass movement was grouped into 3 clusters for each receptor point. Major directions for air mass movements originated from the southwest (80%) of the CM station, which was predominantly comprised of the forest area. At the NN station, major air mass originated from southern (40%), southwestern (35%) and eastern directions (20%). In total, 60% of the air mass arriving at the NN site originated from agricultural areas, while 35% originated from forest areas. In consideration of fire hotspots and air movement directions, air pollutants in CM were mainly caused by forest burning, while agricultural burning was the dominant source at the NN station.

3.2. $PM_{2.5}$-bound PAHs

3.2.1. PAHs concentrations

Concentrations of $PM_{2.5}$ and individual PAHs analyzed from both stations are presented in Table 3. Average $PM_{2.5}$ concentrations were not found to be significantly different. However, the average total PAHs (tPAHs) concentrations of the NN station were about 1.7 times (2017) and 2.6 times (2018) higher than those of the CM station. Average concentrations of tPAHs obtained at the NN station were 4.45 ± 3.22 ng/m^3 (2017) and 5.21 ± 4.02 ng/m^3 (2018), while those obtained at the CM station were 2.57 ± 1.45 ng/m^3 (2017) and 2.02 ± 1.50 ng/m^3 (2018). However, most high MW PAHs are recognized as carcinogenic compounds, and these were found in high proportions in the PM samples collected in this study (Fig. 6). Based on the number of aromatic rings, 16 PAHs can be divided into five groups, which are distinguished by 2-, 3-, 4-, 5- and 6-ring PAHs. The distribution of PAHs based on the number of benzene rings and individual PAHs at each sampling site are shown in Figs. 7 and 8, respectively. PAHs compositions of $PM_{2.5}$ samples collected from both sampling sites were similar. $PM_{2.5}$-bound PAHs with 4–6 rings were recognized as the major group. These 4-6-ring PAHs are high in MW compounds and were presented in the particle phase. On the other hand, low MW PAHs were presented in low concentrations due to their higher volatility. High MW PAHs were dominate and accounted for >90% of tPAHs. Among 16 PAHs, IND (6-ring compound) was a dominant compound with concentrations ranging from 0.05 to 2.38 ng/m^3 (CM) and 0.10–4.51 ng/m^3 (NN). Moreover, Strong relationships between $PM_{2.5}$ and PAHs concentrations, particularly 5-ring PAHs (BbF, BkF, BaP and DbA) and 6-ring PAHs (IND and BPER), were observed at both sampling sites during the study period ($r = 0.6$–0.7). Moreover, the high extraction efficiency of high MW PAHs might be influenced by the degree of solvent extraction efficiency. Organic solvents, such as acetone, dichloromethane (DCM) and n-hexane, were used in several previous studies (Akyuz and Cabuk, 2010; Bootdee et al., 2016; Wang et al., 2016; Zhai et al., 2016). According to the polarity properties of the extraction solvents and PAHs compounds, 5–6 ring PAHs values were close to those of n-hexane, while 4-ring PAHs values were close to those of DCM. In this case, using DCM:n-hexane (1:1) as an extraction solvent, the efficiency order for PAHs with different rings was 5–6 ring PAHs > 4 ring PAHs ≈ 3 ring PAHs (Zhai et al., 2016). Therefore, ratios of high MW PAHs were applied in this study.

3.2.2. PAHs source identification

The diagnostic ratio of PAHs compositions can be used to identify possible emission sources. The diagnostic ratios were calculated by separating sampling sites and collection years as is shown in Fig. 9. According to PAHs concentration ratios, source identification was focused on high MW PAHs. Higher mass PAHs are notably appreciable constituents in samples of wood soot (Lee et al., 1977; Li and Kamens, 1993). The (IND/IND + BPER) ratio above 0.50 refers to biomass combustion (grass, wood bush) and coal combustion aerosols (Yunker et al., 2002). On the other hand, the ratio at < 0.50 is representative of petroleum emissions (gasoline, kerosene, diesel and crude oil) (Yunker et al., 2002). The values between 0.24 and 0.40 represent vehicle emissions (Li and Kamens, 1993; Rogge et al., 1993; Westerholm and Li, 1994; Yunker et al., 2002). The values between 0.40 and 0.42 were reported for indoor air during periods of wood combustion activities employed for cooking purposes (Orakij et al., 2017). The values of the IND/(IND + BPER) ratio showed in this study were >0.50 and therefore were associated with grass, wood and coal combustion activities. These results agreed with the diagnostic ratios of IND/(IND + BPER), which

Table 3
$PM_{2.5}$ and PAHs concentrations (Mean ± SD) of CM and NN stations.

	2017		2018	
	CM (n = 57)	NN (n = 57)	CM (n = 35)	NN (n = 34)
$PM_{2.5}$ (μg/m^3)	38.25 ± 16.05	37.93 ± 19.11	41.86 ± 21.64	38.11 ± 22.49
PAHs (ng/m^3)				
NAP	**0.069 ± 0.027**	0.085 ± 0.038	**0.001 ± 0.005**	ND
ACY	0.027 ± 0.025	**0.062 ± 0.040**	ND	**0.012 ± 0.015**
ACE	**0.000 ± 0.002**	0.019 ± 0.023	**0.004 ± 0.007**	ND
FLU	**0.021 ± 0.016**	**0.035 ± 0.023**	**0.002 ± 0.004**	**0.002 ± 0.006**
PHE	**0.065 ± 0.034**	0.105 ± 0.035	**0.006 ± 0.017**	0.037 ± 0.038
ANT	**0.037 ± 0.027**	0.076 ± 0.044	**0.001 ± 0.004**	0.026 ± 0.027
FLA	**0.125 ± 0.066**	0.078 ± 0.075	**0.023 ± 0.058**	0.084 ± 0.081
PYR	**0.162 ± 0.094**	0.112 ± 0.105	**0.039 ± 0.087**	0.110 ± 0.117
BaA[a]	**0.143 ± 0.097**	**0.254 ± 0.256**	**0.006 ± 0.009**	**0.051 ± 0.049**
CHR[a]	**0.153 ± 0.095**	**0.231 ± 0.191**	**0.009 ± 0.012**	**0.061 ± 0.054**
BbF[a]	**0.245 ± 0.181**	**0.478 ± 0.394**	**0.123 ± 0.077**	**0.300 ± 0.216**
BkF[a]	**0.264 ± 0.164**	0.545 ± 0.381	**0.161 ± 0.093**	0.445 ± 0.322
BaP[a]	**0.268 ± 0.177**	0.663 ± 0.581	**0.098 ± 0.088**	0.498 ± 0.469
IND[a]	**0.472 ± 0.348**	**1.097 ± 0.733**	**0.761 ± 0.555**	**1.668 ± 1.307**
DbA[a]	0.155 ± 0.094	**0.322 ± 0.206**	0.238 ± 0.443	**0.786 ± 0.703**
BPER	**0.367 ± 0.220**	**0.284 ± 0.499**	**0.550 ± 0.499**	**1.134 ± 0.821**
ncPAHs	**0.873 ± 0.363**	**0.856 ± 0.640**	**0.625 ± 0.428**	**1.404 ± 0.969**
cPAHs	1.699 ± 1.110	3.589 ± 2.676	1.394 ± 1.103	3.810 ± 3.077
tPAHs	2.572 ± 1.450	4.445 ± 3.219	2.019 ± 1.503	5.214 ± 4.020

ND is not detected.
Bold express significant difference ($p < 0.05$) of the same substance between years (2017 and 2018) for each station.
Underlines express similarity ($p > 0.05$) between means of individual parameter between CM and NN stations in the same year.
[a] Carcinogenic PAHs.

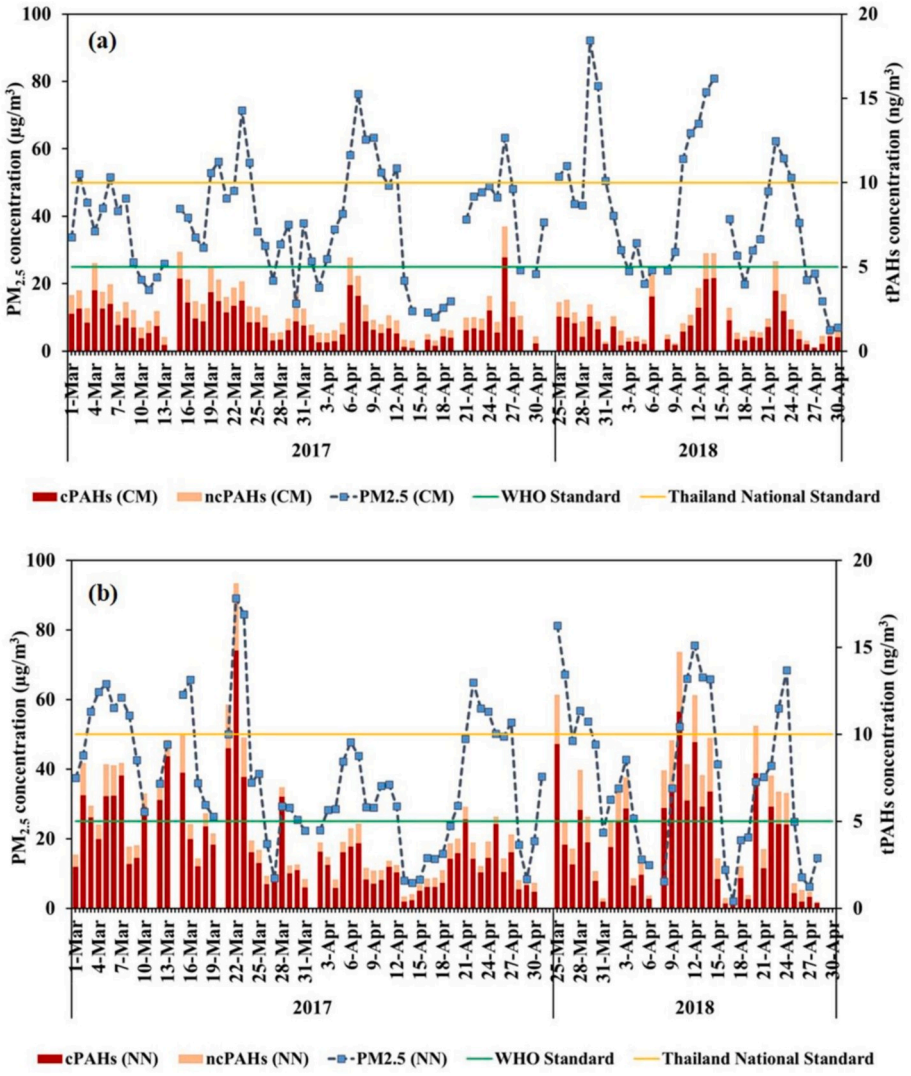

Fig. 6. Daily $PM_{2.5}$, cPAHs and ncPAHs concentrations during the sampling period at (a) CM station and (b) NN station.

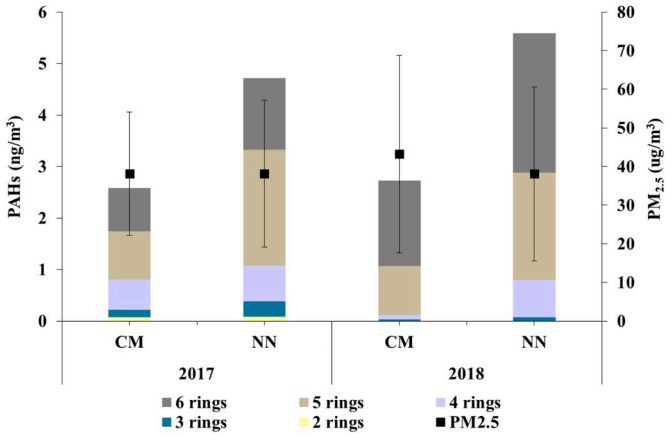

Fig. 7. Spatial distribution of $PM_{2.5}$ and PAHs concentrations based on number of benzene rings.

were 0.88 ± 0.16 (dry season in 2010) and 0.71 ± 0.70 (dry season 2011) and reported in a previous study conducted in the city of Chiang Mai (Wiriya et al., 2013).

The values of the BaA/(BaA + CHR) ratio that were above 0.35 indicated combustion, while values in the range of 0.20–0.35 were associated with mixed sources (either petroleum or combustion). Additionally, values < 0.20 represented petroleum sources (Akyuz and Cabuk, 2010; Finardi et al., 2017; Yunker et al., 2002). The values of the BaA/(BaA + CHR) ratio that were obtained in this study ranged from 0.44 to 0.49. This would imply that the pollutants were generated from biomass combustion. Although the other PAHs isomers were only found in some samples, some of them, such as the PHE/ANT and PRY/FLA ratios, were be calculated. The values of the PHE/ANT ratio (1.53–1.75) were much lower than those of the ratio of ambient air collected from the rural area (5.7–6.0) and the roadside (4.2–6.5) (Boonyatumanond et al., 2007). The PRY/FLA ratios (1.25–1.43) were within the ranges of both rural (1.06–1.20) and roadside (1.02–1.76) sources (Boonyatumanond et al., 2007). Apart from the PAHs ratios, other signature components, such as K^+ and levoglucosan, can be used to indicate biomass combustion sources during episodes of haze pollution in South East Asia (SEA) (Khamkaew et al., 2016; Thepnuan et al., 2018). In this study, the ratio of some significant PAHs can also be used to indicate that biomass burning is a major source of air pollution during episodes of smoke haze in this region. Meanwhile, pollutants from traffic emissions, particularly gasoline engines and internal combustion, might also contribute to air quality.

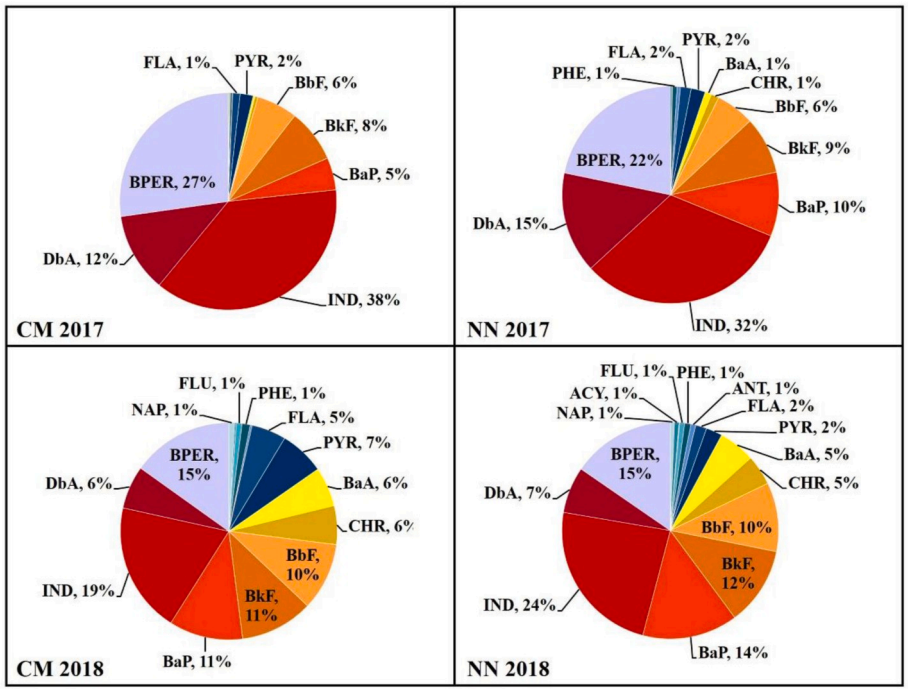

Fig. 8. Ratios of individual PAHs compositions.

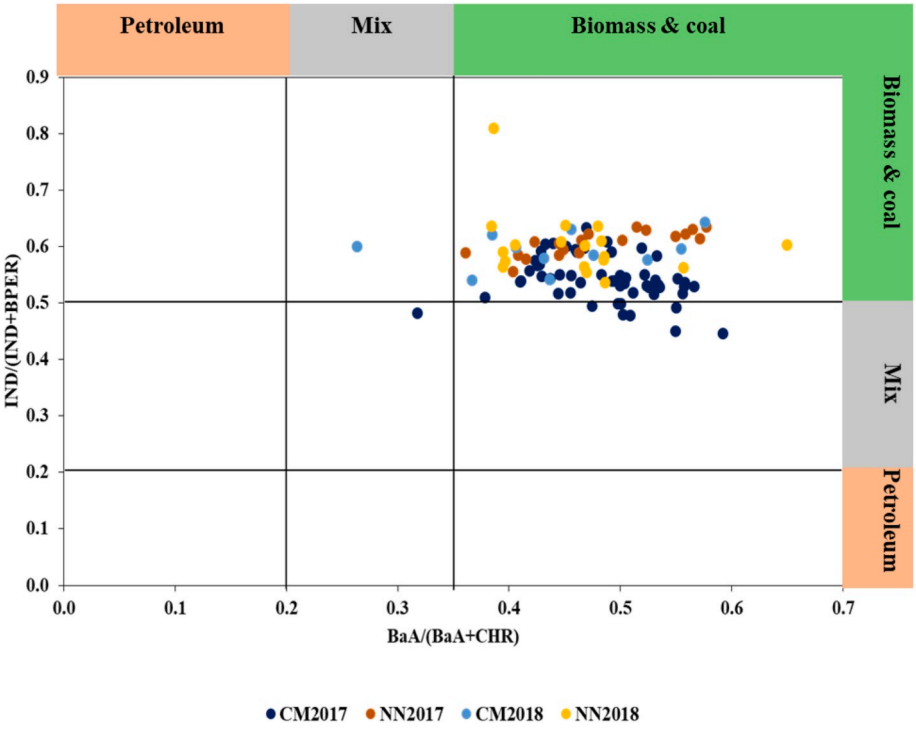

Fig. 9. Diagnostic ratios of isomeric PAHs.

3.2.3. *Health risk assessment*

$PM_{2.5}$ can penetrate more deeply into the human respiratory tract and the toxic compounds that are part of the particles can have severe health impacts. PAHs are recognized as carcinogenic compounds and their concentrations can be used for health risk assessments. The toxicity equivalent concentrations (TEQ) that were calculated based on the TEFs (toxic equivalent factors) values of PAHs are shown in Table 4. In this study, TEQ values were calculated from various equations (Cecinato, 1997; Nisbet and Lagoy, 1992; U.S.EPA, 1993) and no significant differences were found. The TEQ values recorded at the NN station were 2.3 and 3.6 times greater than those recorded at the CM station in 2017 and 2018, respectively. According to the $PM_{2.5}$ concentrations, these results were considerably lower than those recorded in the dry season in 2010 (TEQ = 3.28–3.70), but were slightly higher than those recorded in the dry season in 2011 (TEQ = 0.23–0.26) in the Chiang Mai city (Wiriya et al., 2013).

Table 4
Values of Toxicity equivalent concentrations (TEQ) and inhalation cancer risk (ICR) based on PAHs concentrations at CM and NN stations in 2017 and 2018.

Risk assessment	References	2017		2018	
		CM	NN	CM	NN
TEQ	Nisbet and Lagoy (1992)	0.54 ± 0.34	1.23 ± 0.95	0.45 ± 0.54	1.54 ± 1.36
ICR	WHO (2000)	4.71×10^{-5}	$\mathbf{1.07 \times 10^{-4}}$	3.88×10^{-5}	$\mathbf{1.34 \times 10^{-4}}$
	OEHHA (2003)	5.95×10^{-7}	1.35×10^{-6}	4.91×10^{-7}	1.70×10^{-6}
TEQ	U.S.EPA (1993)	0.44 ± 0.28	1.03 ± 0.82	0.32 ± 0.36	1.16 ± 1.02
ICR	WHO (2000)	3.85×10^{-5}	8.97×10^{-5}	2.80×10^{-5}	$\mathbf{1.01 \times 10^{-4}}$
	OEHHA (2003)	4.87×10^{-7}	1.13×10^{-6}	3.54×10^{-7}	1.27×10^{-6}
TEQ	Cecinato (1997)	0.54 ± 0.34	1.22 ± 0.94	0.44 ± 0.54	1.53 ± 1.35
ICR	WHO (2000)	4.67×10^{-5}	$\mathbf{1.07 \times 10^{-4}}$	3.83×10^{-5}	$\mathbf{1.33 \times 10^{-4}}$
	OEHHA (2003)	5.90×10^{-7}	1.35×10^{-6}	4.85×10^{-7}	1.68×10^{-6}

Bold is classified as high potential cancer risk. According to guideline of ICR values, 10^{-6} of ICR values represents a lower-bound zero risk and $>10^{-4}$ of ICR indicates as high potential cancer risk (Liao and Chiang, 2006).

The average TEQ value was used to calculate the inhalation cancer risk (ICR) and figures were compared among different stations. The ICR of a 70-year lifetime was calculated based on the WHO guidelines (WHO, 2000) and CalEPA (OEHHA, 2003) and is shown in Table 4. The values of ICR for the CM station were 10^{-5} (WHO) and 10^{-7} (CalEPA), while those for the NN station were 10^{-5} - 10^{-4} (WHO) and 10^{-6} (CalEPA). According to the relevant guidelines, ICR values from these two guideline values were different by approximately 100 times due to the IUR_{BaP} values. This differences in the ICR values allowed researchers to estimate the cancer risk incurred from PAHs inhalation, i.e. in 2017 at the CM station. With regard to this, ICR values were 10^{-5} (WHO) and 10^{-7} (CalEPA) and were associated with a medium risk and a low risk of cancer, respectively.

In 2018 at the NN station, 10 in 100,000 people may face the threat of developing cancer if they were exposed to 1 ng/m^3 TEQ over 70 years. Generally, the potential risk is between 10^{-6} to 10^{-4} of the ICR values. The value of 10^{-6} for the ICR value represents a lower-bound zero risk, while the value greater than 10^{-4} of ICR indicates a high potential cancer risk (Liao and Chiang, 2006). The calculated ICR values that were based on concentrations of $PM_{2.5}$ bound PAHs revealed that the NN station was classified as a high-risk region, while the CM station was categorized as a medium-risk location for the inhalation of PAHs. In comparison with the findings of a study by Pongpiachan (2016) that was conducted in 2013 in 9 provinces in Northern Thailand, the ICR values were obviously lower than in this study, which could have been due to the conditions associated with the different years of study, as well as the different sampling locations. The results from our study suggest that it is necessary to control open burning and traffic loading in order to reduce the health risks associated with PAHs in the dry season. Moreover, PAHs and other toxic pollutants should be considered more of a concern with regard to the air quality index and in terms of the serious potential health risks they represent.

4. Conclusion

According to the patterns of $PM_{2.5}$ concentrations (2012–2019) recorded in two locations of our study site, it can be concluded that the implementation of the zero-burning policy had an impact on the patterns and incidences of open burning. During the period of implementation, open burning activities, both in terms of fire hotspot counts and areas burned, were lower than before the implementation of the policy. However, the policy of limiting open burning was expanded from a 2-month period (mid Feb-mid April) to about a 3-month-long period (mid-Feb–mid-May) and was associated with lower concentrations of $PM_{2.5}$. According to the implementation of the zero-burning policy in the years from 2016 to 2019, patterns of $PM_{2.5}$ concentrations corresponded to the fire hotspot counts. In this study, the patterns of ambient $PM_{2.5}$ concentrations recorded in the dry season of the last two years (2017–2018) were different from those of the previous years. $PM_{2.5}$ concentrations tended to fluctuate throughout the haze period and increased again after the middle of April, which was at the end of the policy implementation period. Moreover, climate conditions, including the ENSO cycle and relevant meteorological conditions, were the main factors affecting $PM_{2.5}$ concentration levels. Low levels of $PM_{2.5}$ recorded during the dry season were observed during both sampling years because of the La Niña phenomenon. However, the assessment of $PM_{2.5}$ levels is not enough to satisfactorily classify air quality because the various toxic compounds involved are contained in the particles, which can further promote the risk of human exposure. In this study, we found similar $PM_{2.5}$ concentrations but different PAHs concentrations at the two sampling locations. Average tPAHs concentrations of the NN station were higher than those of the CM station for both years of the study period. According to land use activities and air mass movements, forest and agricultural burning are the major sources of air pollution for the CM and NN collection sites, respectively. This outcome corresponded with the diagnostic ratios of some PAHs i.e. IND/(IND + BPER) and BaA/(BaA + CHR), which can be used to identify the associated source of biomass combustion. Nevertheless, high PAHs concentrations can lead to high values of TEQ representing increased levels of risk from PAHs inhalation. In this case, $PM_{2.5}$ exposure at the NN station was more hazardous than that which was recorded at the CM station for both years. Therefore, toxic chemical compounds should be of great concern in estimating and assessing air quality. Additionally, regulations involving emission control (biomass combustion) should be put in place in order to reduce the health risks associated with air pollutants during the dry season in SEA.

Declaration of competing interest

The authors declare that they have no known competing financial interests or personal relationships that could have appeared to influence the work reported in this paper.

CRediT authorship contribution statement

Nuttipon Yabueng: Methodology, Validation, Formal analysis, Investigation, Writing - original draft, Visualization. **Wan Wiriya:** Conceptualization, Project administration. **Somporn Chantara:** Conceptualization, Resources, Writing - review & editing, Visualization, Supervision, Project administration, Funding acquisition.

Acknowledgments

Funding for this research study was granted by the National Research Council of Thailand (NRCT) via the Haze Free Thailand Project and via the Graduate School, Chiang Mai University (2019) and the Science

Achievement Scholarship of Thailand. This work was also partially supported by Chiang Mai University. Data on $PM_{2.5}$ obtained from the PCD, Thailand, are gratefully acknowledged.

Appendix A. Supplementary data

Supplementary data to this article can be found online at https://doi.org/10.1016/j.atmosenv.2020.117485.

References

Hamburger, T., Matisāns, M., Tunved, P., Ström, J., Calderon, S., Hoffmann, P., Hochschild, G., Gross, J., Schmeissner, T., Wiedensohler, A., Krejci, R., 2013. Long-term in situ observations of biomass burning aerosol at a high altitude station in Venezuela – sources, impacts and interannual variability. Atmos. Chem. Phys. 13, 9837–9853.

Akyuz, M., Cabuk, H., 2010. Gas-particle partitioning and seasonal variation of polycyclic aromatic hydrocarbons in the atmosphere of Zonguldak, Turkey. Sci. Total Environ. 408, 5550–5558.

Armstrong, B., Tremblay, C., Baris, D., Thériault, G., 1994. Lung cancer mortality and polynuclear aromatic hydrocarbons: a case-cohort study of aluminum production workers in Arvida, Quebec, Canada. Am. J. Epidemiol. 139, 250–262.

Bi, X., Sheng, G., Peng, P.a., Chen, Y., Zhang, Z., Fu, J., 2003. Distribution of particulate- and vapor-phase n-alkanes and polycyclic aromatic hydrocarbons in urban atmosphere of Guangzhou, China. Atmos. Environ. 37, 289–298.

Boonyatumanond, R., Murakami, M., Wattayakorn, G., Togo, A., Takada, H., 2007. Sources of polycyclic aromatic hydrocarbons (PAHs) in street dust in a tropical Asian mega-city, Bangkok, Thailand. Sci. Total Environ. 384, 420–432.

Bootdee, S., Chantara, S., Prapamontol, T., 2016. Determination of PM2.5 and polycyclic aromatic hydrocarbons from incense burning emission at shrine for health risk assessment. Atmos. Pollut. Res. 7, 680–689.

Boström, C.-E., Gerde, P., Hanberg, A., Jernström, B., Johansson, C., Kyrklund, T., Rannug, A., Törnqvist, M., Victorin, K., Westerholm, R., 2002. Cancer risk assessment, indicators, and guidelines for polycyclic aromatic hydrocarbons in the ambient air. Environ. Health Perspect. 110, 451.

Castellano, A.V., Cancio, J.L., Alemán, P.S., Rodríguez, J.S., 2003. Polycyclic aromatic hydrocarbons in ambient air particles in the city of Las Palmas de Gran Canaria. Environ. Int. 29, 475–480.

Cecinato, A., 1997. Polynuclear aromatic hydrocarbons (PAH), Benzo (a) pyrene (BaPY) and nitrated-PAH (NPAH) in suspended particulate matter. Ann. Chim. 87, 483–496.

Chantara, S., Sillapapiromsuk, S., Wiriya, W., 2012. Atmospheric pollutants in Chiang Mai (Thailand) over a five-year period (2005–2009), their possible sources and relation to air mass movement. Atmos. Environ. 60, 88–98.

Chantara, S., Thepnuan, D., Wiriya, W., Prawan, S., Tsai, Y.I., 2019. Emissions of pollutant gases, fine particulate matters and their significant tracers from biomass burning in an open-system combustion chamber. Chemosphere 224, 407–416.

Danielsen, P.H., Loft, S., Kocbach, A., Schwarze, P.E., Møller, P., 2009. Oxidative damage to DNA and repair induced by Norwegian wood smoke particles in human A549 and THP-1 cell lines. Mutat. Res. Genet. Toxicol. Environ. Mutagen 674, 116–122.

Duan, J., Bi, X., Tan, J., Sheng, G., Fu, J., 2007. Seasonal variation on size distribution and concentration of PAHs in Guangzhou city, China. Chemosphere 67, 614–622.

Feilberg, A., Poulsen, M.W.B., Nielsen, T., Skov, H., 2001. Occurrence and sources of particulate nitro-polycyclic aromatic hydrocarbons in ambient air in Denmark. Atmos. Environ. 35, 353–366.

Finardi, S., Radice, P., Cecinato, A., Gariazzo, C., Gherardi, M., Romagnoli, P., 2017. Seasonal variation of PAHs concentration and source attribution through diagnostic ratios analysis. Urban Clim. 22, 19–34.

Hanedar, A., Alp, K., Kaynak, B., Baek, J., Avsar, E., Odman, M.T., 2011. Concentrations and sources of PAHs at three stations in Istanbul, Turkey. Atmos. Res. 99, 391–399.

Hassanvand, M.S., Naddafi, K., Faridi, S., Nabizadeh, R., Sowlat, M.H., Momeniha, F., Gholampour, A., Arhami, M., Kashani, H., Zare, A., 2015. Characterization of PAHs and metals in indoor/outdoor PM10/PM2. 5/PM1 in a retirement home and a school dormitory. Sci. Total Environ. 527, 100–110.

Khalili, N.R., Scheff, P.A., Holsen, T.M., 1995. PAH source fingerprints for coke ovens, diesel and, gasoline engines, highway tunnels, and wood combustion emissions. Atmos. Environ. 29, 533–542.

Khamkaew, C., Chantara, S., Janta, R., Pani, S.K., Prapamontol, T., Kawichai, S., Wiriya, W., Lin, N.-H., 2016. Investigation of biomass burning chemical components over northern Southeast Asia during 7-SEAS/BASELInE 2014 campaign. Aerosol and Air Qual. Res. 16, 2655–2670.

Kim, K.H., Lee, S.-B., Woo, D., Bae, G.-N., 2015. Influence of wind direction and speed on the transport of particle-bound PAHs in a roadway environment. Atmos. Pollut. Res. 6, 1024–1034.

Lee, M.L., Prado, G.P., Howard, J.B., Hites, R.A., 1977. Source identification of urban airborne polycyclic aromatic hydrocarbons by gas chromatographic mass spectrometry and high resolution mass spectrometry. Biomed. Mass Spectrom. 4, 182–186.

Li, C.K., Kamens, R.M., 1993. The use of polycyclic aromatic hydrocarbons as source signatures in receptor modeling. Atmos. Environ. 27, 523–532.

Liao, C.M., Chiang, K.C., 2006. Probabilistic risk assessment for personal exposure to carcinogenic polycyclic aromatic hydrocarbons in Taiwanese temples. Chemosphere 63, 1610–1619.

Liu, D., Lin, T., Syed, J.H., Cheng, Z., Xu, Y., Li, K., Zhang, G., Li, J., 2017. Concentration, source identification, and exposure risk assessment of PM2.5-bound parent PAHs and nitro-PAHs in atmosphere from typical Chinese cities. Sci. Rep. 7, 10398.

Manoli, E., Kouras, A., Samara, C., 2004. Profile analysis of ambient and source emitted particle-bound polycyclic aromatic hydrocarbons from three sites in northern Greece. Chemosphere 56, 867–878.

Nisbet, I.C., Lagoy, P.K., 1992. Toxic equivalency factors (TEFs) for polycyclic aromatic hydrocarbons (PAHs). Regulat. Toxicol. Pharmacol. Therapeut. 16, 290–300.

OEHHA, 2003. Air Toxics Hot Spots Program Risk Assessment Guidelines: the Air Toxics Hot Spots Program Guidance Manual for Preparation of Health Risk Assessments, California. Office of Environmental Health Hazard Assessment.

Orakij, W., Chetiyanukornkul, T., Kasahara, C., Boongla, Y., Chuesaard, T., Furuuchi, M., Hata, M., Tang, N., Hayakawa, K., Toriba, A., 2017. Polycyclic aromatic hydrocarbons and their nitro derivatives from indoor biomass-fueled cooking in two rural areas of Thailand: a case study. Air Qual. Atmos. Health 10, 747–761.

Pani, S.K., Lin, N.-H., Chantara, S., Wang, S.-H., Khamkaew, C., Prapamontol, T., Janjai, S., 2018. Radiative response of biomass-burning aerosols over an urban atmosphere in northern peninsular Southeast Asia. Sci. Total Environ. 633, 892–911.

Pongpiachan, S., 2016. Incremental lifetime cancer risk of PM2. 5 bound polycyclic aromatic hydrocarbons (PAHs) before and after the wildland fire episode. Aerosol Air Qual. Res 16, 2907–2919.

Punsompong, P., Chantara, S., 2018. Identification of potential sources of PM10 pollution from biomass burning in northern Thailand using statistical analysis of trajectories. Atmos. Pollut. Res. 9, 1038–1051.

Ravindra, K., Wauters, E., Van Grieken, R., 2008. Variation in particulate PAHs levels and their relation with the transboundary movement of the air masses. Sci. Total Environ. 396, 100–110.

Rogge, W.F., Hildemann, L.M., Mazurek, M.A., Cass, G.R., Simoneit, B.R., 1993. Sources of fine organic aerosol. 2. Noncatalyst and catalyst-equipped automobiles and heavy-duty diesel trucks. Environ. Sci. Technol. 27, 636–651.

Sarigiannis, D.A., Karakitsios, S.P., Zikopoulos, D., Nikolaki, S., Kermenidou, M., 2015. Lung cancer risk from PAHs emitted from biomass combustion. Environ. Res. 137, 147–156.

Schnelle-Kreis, J., Gebefügi, I., Welzl, G., Jaensch, T., Kettrup, A.J.A.E., 2001. Occurrence of Particle-Associated Polycyclic Aromatic Compounds in Ambient Air of the City of Munich, vol. 35, pp. S71–S81.

Thepnuan, D., Chantara, S., Lee, C.T., Lin, N.H., Tsai, Y.I., 2018. Molecular markers for biomass burning associated with the characterization of PM2.5 and component sources during dry season haze episodes in Upper South East Asia. Sci. Total Environ. 658, 708–722.

U.S.EPA, 1993. Provisional Guidance for Quantitative Risk Assessment of Polycyclic Aromatic Hydrocarbons. US Environmental Protection Agency, Research Triangle Park. NC EPA-600/R-93/089.

U.S.EPA, 2005. Guidelines for Carcinogen Risk Assessment. Risk Assessment Forum, Washington DC.

Wang, Q., Liu, M., Yu, Y., Li, Y., 2016. Characterization and source apportionment of PM2.5-bound polycyclic aromatic hydrocarbons from Shanghai city, China. Environ. Pollut. 218, 118–128.

Wang, C., Wu, S., Zhou, S., Shi, Y., Song, J., 2017. Characteristics and source identification of polycyclic aromatic hydrocarbons (PAHs) in urban soils: a review. Pedosphere 27, 17–26.

Westerholm, R., Li, H., 1994. A multivariate statistical analysis of fuel-related polycyclic aromatic hydrocarbon emissions from heavy-duty diesel vehicles. Environ. Sci. Technol. 28, 965–972.

WHO, 2000. Air Quality Guideline for Europe, second ed. WHO, Copenhagen. WHO Regional Publications 2000: European Series, No.91.

Wiriya, W., Prapamontol, T., Chantara, S., 2013. PM10-bound polycyclic aromatic hydrocarbons in Chiang Mai (Thailand): seasonal variations, source identification, health risk assessment and their relationship to air-mass movement. Atmos. Res. 124, 109–122.

Yunker, M.B., Macdonald, R.W., Vingarzan, R., Mitchell, R.H., Goyette, D., Sylvestre, S., 2002. PAHs in the Fraser River basin: a critical appraisal of PAH ratios as indicators of PAH source and composition. Org. Geochem. 33, 489–515.

Zhai, Y., Li, P., Zhu, Y., Xu, B., Chen, H., Zeng, G., 2016. Effects of Solvent and Time on Extraction Efficiency of Ultrasonic Extraction for Polycyclic Aromatic Hydrocarbons from Atmospheric Particulate Matter.

Zhang, Y., Tao, S., 2009. Global atmospheric emission inventory of polycyclic aromatic hydrocarbons (PAHs) for 2004. Atmos. Environ. 43, 812–819.